RIGA TECHNICAL UNIVERSITY

Armands Ancāns

BODY SENSOR NETWORK FOR ITS SURFACE SHAPE RECONSTRUCTION

Summary of the Doctoral Thesis

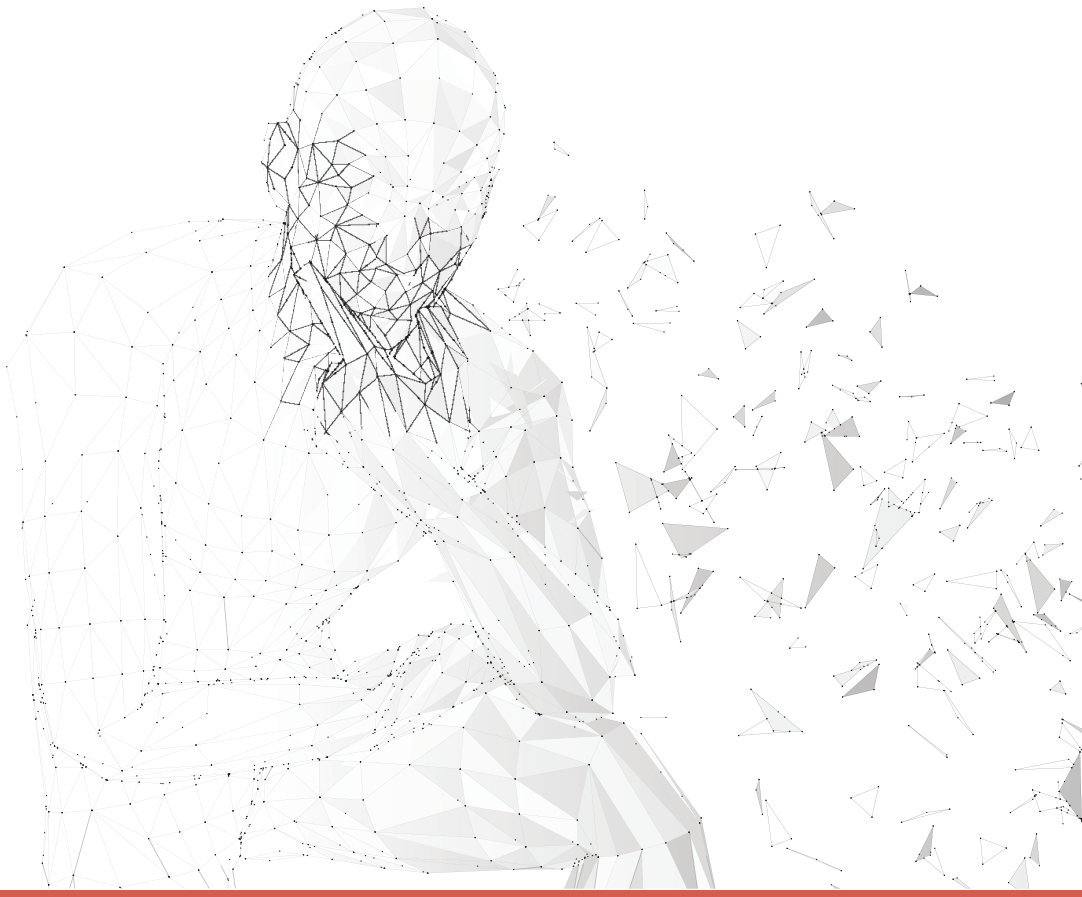

RTU Press
Riga 2023

RIGA TECHNICAL UNIVERSITY
Faculty of Electronics and Telecommunications
Institute of Microwave Engineering and Electronics

Armands Ancāns
Student of the Doctoral study program "Electronics"

BODY SENSOR NETWORK FOR ITS SURFACE SHAPE RECONSTRUCTION

Summary of the Doctoral Thesis

Scientific supervisor
Dr. sc. comp.
MODRIS GREITĀNS

RTU Press
Riga 2023

Ancāns, A. Body Sensor Network for Its Surface Shape Reconstruction. Summary of the Doctoral Thesis. – Riga: RTU Press, 2023. – 45 p.

Published in accordance with the decision of the Promotion Council “RTU P-08” of 6 April 2023, Minutes No. 21.

https://doi.org/10.7250/9789934229251
ISBN 978-9934-22-925-1 (pdf)

DOCTORAL THESIS PROPOSED TO RIGA TECHNICAL UNIVERSITY FOR THE PROMOTION TO THE SCIENTIFIC DEGREE OF DOCTOR OF SCIENCE

To be granted the scientific degree of Doctor of Science (Ph. D.), the present Doctoral Thesis has been submitted for the defence at the open meeting of RTU Promotion Council on 16 June 2023 at 11.00 at the Faculty of Electronics and Telecommunications of Riga Technical University, 12 Azenes Street, Room 201.

OFFICIAL REVIEWERS

Professor Dr. sc. ing. Aleksandrs Grakovskis
Transport and Telecommunication Institute, Latvia

Professor Dr. sc. ing. Dmitrijs Pikuļins
Riga Technical University

Emeritus Professor Dr. sc. ing. Mart Min
Tallinn University of Technology, Estonia

DECLARATION OF ACADEMIC INTEGRITY

I hereby declare that the Doctoral Thesis submitted for the review to Riga Technical University for the promotion to the scientific degree of Doctor of Science (Ph. D.) is my own. I confirm that this Doctoral Thesis had not been submitted to any other university for the promotion to a scientific degree.

Armands Ancāns ……. (signature)
Date: ……

The Doctoral Thesis has been written in Latvian. It consists of an Introduction, 5 chapters, conclusions, 33 figures, 5 tables, 4 appendices; the total number of pages is 62, not including appendices. The Bibliography contains 52 titles.

TABLE OF CONTENTS

NOMENCLATURE

2D	two dimensions
3D	three dimensions
ADDR	UART address bit frame configuration
BCC	body-coupled communication
BLE	Bluetooth Low Energy
BSN	body sensor network
BT	Bluetooth
CSV	comma-separated values
I2C	inter-integrated circuit
ICP	iterative closest point
ID	identification number
IDLE	UART idle bit frame configuration
IMU	inertial measurement unit
MCU	microcontroller unit
MEMS	micro-electro-mechanical system
Rx	interface receive input
SPI	serial peripheral interface
Tx	interface transmit output
UART	universal asynchronous receiver-transmitter
VCC	positive supply voltage
VQF	versatile quaternion-based filter

ABBREVIATIONS

α	angle measured with respect to the horizontal axis
$\boldsymbol{C}$	set of curve points
$\boldsymbol{C}_{\mathbf{avg}}$	weighted average value of the curve vector
$\boldsymbol{D}_{\mathbf{off}}$	offset vector of the curve
$\boldsymbol{R_k}$	the rotation matrices associated with the k-th segment of the zigzag line structure.
$\boldsymbol{v_k^*}$	the reference states associated with the k-th segment of the zigzag line structure.
$\boldsymbol{v_k}$	vectors comprising the zigzag structures, indexed by k. See Fig. 2.4.
η	efficiency of symbol transmission
λ	stretching coefficient of simulated zigzag structures
σ	Standard deviation
d	Euclidean distance
f_b	symbol rate of the interface
K	total number of sensors
k	sensor index
K_{gen}	the number of random samples used for 2D curve synthesis
L	total length of the curve
L_k	the length of the vectors forming the zigzag line structures with index k.
M	number of connection points
m	connection point index
n_{data}	number of binary data symbols in the message
n_{nodes}	number of nodes connected to the network
N_{rand}	number of random simulations
n_{sens}	number of sensors in the simulated zigzag structure
s	arc-length parameter of the curve
s_{conn}	length of the curve between connection points of the simulated zigzag structure

t_b time taken to transmit one binary symbol

$t_{protocol}$ time required to transmit data symbols according to the protocol

u, v parameters characterizing a parametric surface

w coefficients of point weights of lines

GENERAL DESCRIPTION OF THE RESEARCH

Relevance

The field of human body shape and movement analysis has been the subject of rapidly growing research interest, as it offers a wealth of versatile information. In fact, according to the esteemed SCOPUS scientific publication database, there are over 76,000 documents on the topic of "human body movements" from 1890 to 2021, with a very sharp increase in recent years. Understanding the intricacies of human body shape and movement not only sheds light on the operation of the musculoskeletal system, but also on the sleep, human communication, and development of nervous system, opening up new doors for sports, rehabilitation, and medical diagnosis.

Digital reconstruction of human movements has become increasingly important, as it has numerous applications in a variety of fields. These range from creating natural-looking digital content for films and video games, to planning the movements of robotic systems to move like humans, and developing intuitive human-computer interfaces. While body sensors are mostly associated with the human body, they can also be utilized for other bodies that require similar mobility and non-intrusive operation, such as soft robotics systems and construction safety monitoring.

Body shape and movement can be assessed using various approaches that can be broadly categorized into two groups based on the type of equipment used. The first group involves methods that rely on external equipment, such as stereo cameras, *LiDAR* systems, and touch-sensitive probes. These methods offer high precision, but their operational range is limited, and environmental factors such as visibility and object occlusion can adversely affect their performance.

In contrast, the second group of approaches utilizes equipment that is attached to the body of interest, and it is more suitable for challenging environments such as crowds, urban areas, or natural settings, where providing the necessary conditions for external equipment may be difficult. This group includes mobile body sensor systems that leverage mechanical deformation and inertial sensors. These methods offer greater flexibility and robustness, making them a suitable choice for practical applications in real-world settings.

As material science advances, the precision and feasibility of mechanical deformation sensors integrated into clothing continue to improve. However, these sensors face limitations in accurately tracking moderate to high amplitude movements. In contrast, inertial micro-electro-mechanical systems (MEMS) have emerged as a promising alternative for monitoring body movements in mobile sensor systems. MEMS sensors are extremely compact and can be discreetly integrated into clothing or accessories, making them a practical choice for everyday use.

The results of body shape and movement reconstruction using MEMS sensors offer high precision for both static and dynamic movements, comparable to the precision of optical systems [10]. This makes MEMS sensors an excellent option for monitoring body

movements in various settings, including those where external equipment may not be feasible.

While several methods exist for body shape reconstruction using MEMS sensors, they are primarily based on local orientation measurements obtained with MEMS inertial sensors. However, orientation data alone is insufficient for determining the spatial coordinates that characterize the shape of an object. To reconstruct the geometric shape of an object accurately, the relative distances between sensor nodes must be known [21]. Special sensors designed for precise distance determination significantly increase the cost and complexity of such systems, making them impractical for many applications.

As a result, in reviewed systems for body shape reconstruction, the distance between sensors is fixed and considered constant [10]. While this simplifies the system design and reduces cost, it limits the applicability of these systems to objects that are not subjected to stretching. Therefore, a more sophisticated approach is required for the reconstruction of complex body shapes subjected to bending and stretching deformation.

Research objectives

The goal of the Thesis is to design and develop a scalable and efficient body sensor system capable of accurately reconstructing stretchable and bendable body shapes. To achieve this, a novel methodology is proposed, utilizing orientation sensors in structures to reconstruct the geometric shape of the body accurately. This approach enables the reconstruction of points that characterize the body's form, even if they are stretched or bent, without affecting the distances between the sensors on the structure's surface.

However, detailed reconstruction of the body shape requires a complex and large sensor network, which presents challenges in terms of efficient data collection. Therefore, the research also presents a novel approach to optimize sensor data collection, involving a customized system architecture and a new communication protocol. These improvements enable efficient data transfer and minimize energy consumption, making the proposed body sensor system both scalable and efficient.

To accomplish the research objectives, the following tasks have been identified:

- Conduct a literature review of existing methods for reconstructing the geometric shape of the body using sensors physically attached to the body.
- Investigate the feasibility of the proposed approach for reconstructing the body's geometric shape and compare it with other currently known methods.
- Conduct a literature review of communication solutions for efficient data acquisition from a large number of sensors on the body.
- Evaluate the performance of the proposed data acquisition approach for obtaining data from body sensors for shape reconstruction using inertial sensors in structures.
- Develop an experimental set-up to determine the coordinates of points that characterize the geometric forms of the body and investigate sensor data acquisition methods.

- Summarize the experimental results obtained and test hypotheses regarding the feasibility of the proposed method for determining the coordinates of points characterizing the body shape and the applicability of the proposed architecture for data acquisition from a body sensor network with a large number of functionally equivalent nodes.

Research methodology

To accomplish the defined tasks of the Thesis, the following research methodology was utilized. Firstly, a literature analysis was conducted to gain insight into published materials related to the research problem. Analytical modeling is then utilized to evaluate the theoretical foundations and limitations of the proposed communication solutions. Numerical simulations are conducted to investigate the impact of reconstruction method parameters on the accuracy of the reconstructed body shape. Finally, experimental studies are carried out to validate the proposed approaches for body shape reconstruction and data acquisition from body sensors.

Scientific novelty and key findings

The scientific novelty of this work comprises two parts:

- The development and testing of a new approach that enables the reconstruction of points characterizing the geometric shape of an object using orientation sensors in stretchable structures.
- The development and testing of a new approach that facilitates the acquisition of data from a body sensor network with a large number of functionally equivalent nodes using low-energy communication interfaces spread across microcontrollers (MCUs).

In the simulations conducted to reconstruct line points using zigzag structures, the accuracy of point reconstruction was evaluated while considering the influence of the zigzag structure and sensor parameters. These results were compared with a traditional approach where sensors are placed directly on the body instead of on the structure. Through these comparisons, significant characteristics of the proposed approach were identified, including the following:

- The proposed approach is less influenced by the complexity of the body shape, resulting in more accurate reconstruction results.
- As sensor errors decrease, the error in the reconstructed points converges to zero regardless of the complexity of the body shape for zigzag structures.
- The allowable stretch of zigzag structures has a proportional impact on the error of point reconstruction.

In the experimental studies, a zigzag structure was developed to identify 12 characteristic points of the arm shape. The accuracy of the proposed method was evaluated by

comparing it with the Optitrack™ infra-red camera system, which was used to reconstruct the arm shape in different poses. The results showed an average difference of 19.9 mm between the reconstructed points, measured as the Euclidean distance.

The proposed approach for body sensor data acquisition offers efficient communication with large groups of sensors containing functionally identical nodes. It facilitates power supply, synchronization of node readings, minimal constraints on the physical topology of network nodes, and system scalability. In addition, the approach can be implemented using standard communication interfaces and low-power consumption MCUs.

The proposed approach for acquiring sensor data in the developed experimental set-up is implemented through a 3-wire connection network that transmits both data signals and power supply voltage. The created wire network is utilized to collect data from a group of 26 inertial sensors at a sampling rate of 50 times per second. Upon evaluating the performance of the communication protocol, it was found that the sensor reading frequency can practically be increased up to 93 Hz using the sensor nodes utilized in the set-up, which is approximately 64 % of the theoretical maximum value of the specific protocol (144.9 Hz).

Theses to be defended

The following theses were formulated and demonstrated in the Doctoral Thesis:

1. The proposed approach is applicable for reconstructing the surface shape of the body in cases of both stretching and bending deformations, as long as the length of the cord between the structure connection points does not exceed the length of the structure segment connecting these points.

2. Compared to using orientation sensors directly on the body, the proposed approach of utilizing orientation sensors in zigzag structures connected to specific points on the body results in less dependence on the body shape for body shape reconstruction.

3. The proposed half-duplex wire communication protocol reduces the required overhead for communication with grouped nodes proportionally to the number of grouped nodes.

Practical application and published works

The Doctoral Thesis was developed at the Institute of Electronics and Computer Science, and the proposed approaches were created through the development of technologies for determining body shape using wearable inertial sensors in several European and Latvian projects:

- National Research Programme “Cyber-physical systems, ontologies and biophotonics for safe & smart city and society” (VPP SOPHIS) project No. 1 “Development

of technologies for cyber physical systems with applications in medicine and smart transport" (KiFiS).
- FLAG-ERA project "Frictionless Energy Efficient Convergent Wearables For Healthcare and Lifestyle Applications" No. ES RTD/2017/21 (CONVERGENCE).
- European Regional Development Fund (ERDF), Measure 1.2.1. Specific support goal "To Increase the Private Sector Investments R & D"; measure 1.2.1.2. "Support for Improvement of Technology Transfer System" project "3D shape sensing fabric" (Nr. KC-L-2017/4 un Nr. KC-PI-2017/25) (3D AUDUMS).
- ERDF Measure 1.2.1. Specific support goal "To Increase the Private Sector Investments R & D"; measure 1.2.1.2. "Support for Improvement of Technology Transfer System" project" project "Sensorial Clothes for Accurate Physical Exercise and Instant Feedback", Nr. KC-PI-2020/42 (SCAPE-IF).
- National Research Programme "Smart Materials, Photonics, Technologies and Engineering Ecosystems" (Nr. VPP-EM-FOTONIKA-2022/1-0001).

The proposed method for reconstructing body shape in this study enables the development of stretchable sensor garments that fit closely to the body and allow for precise determination of body shape and related parameters, such as real-time movement of the skeletal-muscular system or measurements of body part circumference and proportions. This approach has the potential to eliminate the need for pose calibration of inertial motion capture systems and input of individual body proportions. The method presented in this study for reconstructing characteristic points of body shape opens up new possibilities for developing more realistic computer models of the human body that take into account not only the orientation and position of body parts but also plastic body deformations, such as those that occur during breathing. Given the advantages and potential applications of the proposed body shape reconstruction method in product development, a Latvian patent has been written and a patent application No. LVP2021000078 has been submitted to the Latvian Patent Office.

The approach proposed in this study for optimized communication with node groups using minimal wiring is applicable to implementations of wired body sensor networks (BSNs) where communication and real-time data acquisition must be ensured for a large number of BSN nodes. The proposed communication approach can be implemented using widely available low-power MCU wire communication interfaces, thus node development does not require additional specific components. Considering that the proposed approach facilitates the development and integration of wired BSNs into clothing, it has the potential to promote the development of new BSN technologies and products that require data acquisition from a large number of densely deployed sensor nodes.

The results of the Doctoral Thesis are associated with four scientific publications: **[3]**, **[20]**, **[4]**, **[2]**.

Structure of the Thesis

In Chapter 1 of the Thesis, previous studies and technologies for determining body shape with body sensors are reviewed. In Section 1.1 algorithms for determining shape based on orientation sensors are discussed in more detail. Accordingly, the basic principles of operation of inertial sensors, which allow for the determination of the physical orientation of the sensor, are reviewed in Section 1.2. Section 1.3 explores the architectures of BSNs and the methods for acquiring sensor data found in literature, considering the significant number of sensors required for detailed reconstruction of body shape.

In Chapter 2 of the Thesis, a new approach for reconstructing the body shape using orientation sensors integrated into body-attached structures is proposed and explained in detail. Specifically, the case of the zigzag structure, potentially the most suitable for BSN applications, is examined in more detail in Section 2.3.

Considering that the implementation of the proposed method requires real-time data acquisition from a large number of body sensors that may form complex physical topologies, Chapter 3 presents an architecture and a novel communication protocol that enables efficient communication with groups of network nodes while minimizing the number of wires required for connectivity.

At the beginning of Chapter 4, simulations were conducted to validate the proposed method for reconstructing body shape using synthetic data (as discussed in Section 4.1). The section then proceeds to describe the experimental set-up developed for reconstructing the arm shape using sensor nodes embedded in zigzag structures, followed by a comparative study of the set-up reconstructed coordinate points with those obtained from the Optitrack infrared camera system.

Chapter 4 is devoted to the validation of the proposed method for shape reconstruction of the proposed system architecture for sensor data acquisition. In Section 4.1, simulations were carried out to demonstrate shape reconstruction using synthetic data. The subsequent section describes the development of an experimental set-up for reconstructing the shape of the arm through the use of sensor nodes embedded in zigzag structures. This is followed by a comparative study, wherein the reconstructed coordinate points of the set-up are compared to those obtained from the Optitrack infra-red camera system.

The final section of this dissertation presents a summary of the research findings and the conclusions drawn from the study.

1. SENSOR DATA ACQUISITION AND BODY SHAPE RECONSTRUCTION

The purpose of this Chapter is to review and analyze existing techniques for reconstructing body shape using body sensors. Emphasis is given to methods based on orientation sensors and MEMS inertial sensors for their potential high precision. Additionally, published BSN technologies are examined for sensor data acquisition, as the number of sensors required for detailed shape reconstruction can be considerable.

1.1. Methods for body geometric shape reconstruction

After examining various body sensor technologies for body shape reconstruction, MEMS orientation sensors have been identified as the most potentially suitable. These sensors can be manufactured in small sizes, integrated into clothing and accessories, and used for determining high-precision static and dynamic body shapes.

The reconstruction of body shapes using orientation sensor data was initially studied by Nathalie Sprynski [21]. To reconstruct the shape from sensors she proposed a mathematical formulation based on the arc-length parametrization of the curve $\boldsymbol{C}(s) = = [x(s), y(s), z(s)]^\intercal$, where $s \in [0, L]$ and L is the total length of the curve.

Curves that are parametrized by the arc-length have a unit vector derivative, which in 2D is denoted as $\boldsymbol{C}'(s) = [\cos\alpha(s), \sin\alpha(s)]^\intercal$, where $\alpha \in [0,2\pi)$ is the angle between the curve tangent and the horizontal axis (refer to Fig. 1.1). Therefore, the problem of reconstructing a 2D curve from orientation sensor data can be formulated as follows: given samples of the angle function $\alpha_k = \alpha(s_k)$ and corresponding values of the curve parameter s_k, where $k = 1,2,...,K$, find the curve $\boldsymbol{C}(s)$ that satisfies the condition $\boldsymbol{C}'(s_k) = = [\cos\alpha_k, \sin\alpha_k]^\intercal$.

N. Sprynki proposed to solve this by interpolating the samples of the angle function using cubic splines and reconstructing the curve $\boldsymbol{C}(s)$ by numerically integrating the obtained derivative function components:

$$\boldsymbol{C}(s) = \begin{bmatrix} x(s) \\ y(s) \end{bmatrix} = \begin{bmatrix} x_0 + \int_0^s \cos\alpha(t)dt \\ y_0 + \int_0^s \sin\alpha(t)dt \end{bmatrix}, \tag{1.1}$$

where x_0 and y_0 are the coordinates of the reconstruction reference point.

The proposed approach can be expanded to 3D lines [17] and 3D surfaces [21].

The literature presents prototypes for reconstructing the shapes of objects using inertial and magnetic sensors, which are summarized in Table 1.1. In all the considered systems, the inter-sensor distances are fixed and do not permit body stretch deformations.

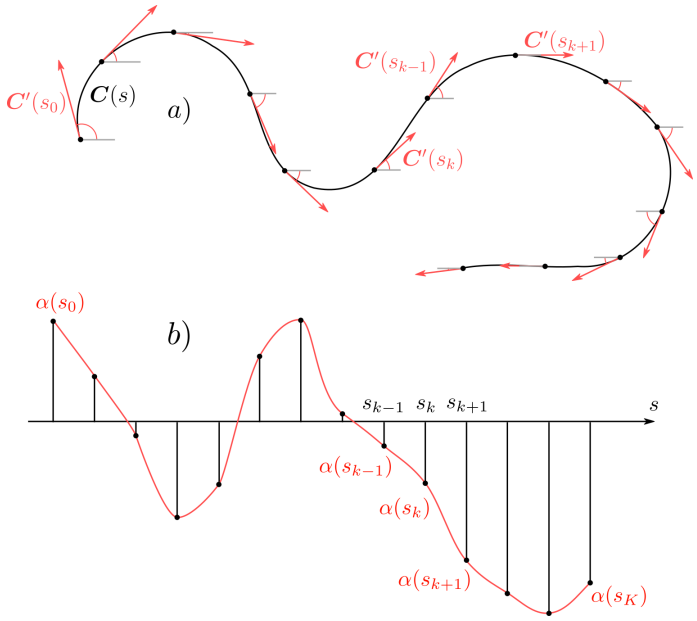

Fig. 1.1. Illustration of curve reconstruction from sensor data: a) curve and its derivative at discrete points s_k; b) angle function $\alpha(s)$, which is reconstructed from discrete readings α_k, corresponding to the angle between vectors of the curve derivative and the horizontal axis.

1.2. Inertial sensors for orientation estimation

Orientation estimation using MEMS inertial sensor nodes (IMUs), which can incorporate accelerometers, gyroscopes, and magnetometers in various combinations, has become a fundamental component of inertial body motion analysis. To date, the VQF (versatile quaternion-based filter) algorithm provides the best results for IMU data fusion and orientation determination, with an average quadratic error in orientation that is almost two times lower than alternative algorithms, according to the literature [12].

1.3. Communication in body sensor networks

One of the most important criteria in body sensor network technologies is freedom of movement and ease of use. Therefore, BSNs primarily use wireless sensor technologies. The only official wireless BSN standard is IEEE 802.15.6 (IEEE Standard for Local and Metropolitan Area Networks – Part 15.6: Wireless Body Area Networks). Despite academic interest, manufacturer-specific solutions or the Bluetooth Low Energy (BLE) protocol, which is widely supported in personal mobile devices, are more commonly used in practice.

There are several challenges in the use of wireless body sensor nodes, including the

Table 1.1
Summary of devices for object shape reconstruction using inertial and magnetic sensors

Device	Sensor placement	Structure
Device for spine shape reconstruction [5]	Fixed	Ribbon
"Morphosense" [16]	Fixed	Ribbon
"Morphopipe" [19]	Fixed	Ribbon
"Morphoshape" [15]	Fixed	Grid
3DCS [11]	Fixed	Grid
Shape sensing fabric [1]	Fixed	Grid

complexity of designing the transmitter and receiver electrical circuits, the need for each node to have a battery or energy harvesting mechanisms from the surrounding environment (such as vibrations, heat, or sunlight), the limited frequency band that needs to be shared with other devices, which can often degrade system performance, and the potential risks to data security, as the transmitted information is easier to intercept. These challenges could potentially be addressed through wired communication approaches described in Section 1.4.

1.4. Overview of microcontroller communication interfaces

In this section, we will examine and compare three main low-power MCU wired communication interfaces for BSN development: inter-integrated circuit (I2C), universal asynchronous receiver-transmitter (UART), and serial peripheral interface (SPI). We will pay particular attention to the number of wires used for interface configurations, wired connection requirements, data transfer rates, and efficiency.

To compare the interfaces and their configurations, analytical expressions will be developed to evaluate the efficiency of symbol transmission η:

$$\eta = \frac{t_b \cdot n_{data}}{t_{protocol}} = \frac{n_{data}}{t_{protocol} \cdot f_b}, \tag{1.2}$$

where $t_{protocol}$ – the time required to transmit data symbols according to the protocol;

t_b – the time required to transmit one symbol;

f_b – the symbol rate of the interface.

I2C

The I2C interface operates on a synchronous, half-duplex serial bus with two unipolar connections: a data line (SDA) and a clock line (SCL). While it is often utilized for creating wired systems with electronic nodes embedded in clothing, as supported by various literature sources [5], [18], [14], there are limitations to using I2C in BSN applications. The parasitic parameters of the bus constrain the length of open collector or open drain

buses and the number of devices that can be connected. Additionally, communication conflicts can arise, and adding or removing nodes during system operation is limited.

According to the signal specifications of the I2C protocol, the efficiency of symbol transmission in basic data exchange procedures is:

$$\eta_{i2c} = \frac{n_{data}}{t_{i2c} \cdot f_b} = \frac{n_{data}}{9 + 1{,}25 \cdot n_{data} + 2{,}5 \cdot 10^{-9} f_b}. \tag{1.3}$$

UART

UART communication operates at the physical layer using two unipolar data lines: a receiving line (Rx) and a transmitting line (Tx). These lines can be utilized for simplex, half-duplex, and full-duplex communication between connected nodes. To encode signals on these lines, push-pull transistor outputs are used, allowing for rapid switching between logical signal levels. When it comes to addressing nodes and separating data blocks, there are two approaches available: idle frames (IDLE) or frames with address bits (ADDR). Assuming a common serial communication configuration with 8 data bits, 1 stop bit, and no parity bits, the efficiency of symbol transmission for n_{data} data symbols using IDLE and ADDR addressing approaches can be expressed as follows:

$$\eta_{uart\_idle} = \frac{n_{data}}{20 + 1{,}25 \cdot n_{data}}, \tag{1.4}$$

$$\eta_{uart\_addr} = \frac{n_{data}}{11 + 1{,}375 \cdot n_{data}}. \tag{1.5}$$

SPI

SPI is a synchronous serial communication interface that utilizes a group of 4 unipolar lines (MISO, MOSI, CLK, CS) for communication. The signals on these lines are encoded using push-pull transistor outputs, which, similar to UART, provide relatively fast switching between logical levels.

Although SPI is not typically used in networks with many sensors because of the excessive wiring, there are modifications such as the enhanced SPI daisy-chain with two wires that can be applied in such situations [9]. Nevertheless, it should be noted that this approach's line topology may not be efficient in complex network physical topologies, as it doesn't make the best use of wiring.

When communicating with a large number of sensor nodes, the SPI half-duplex bus configuration with three wires (MISO/MOSI, CLK, CS) can be utilized. Unlike other interfaces reviewed before, SPI modules do not have an integrated special addressing scheme for half-duplex configuration. However, to enable comparison with other communication protocols, the first eight block symbols can be reserved for addressing. The efficiency of this protocol can then be evaluated as follows:

$$\eta_{spi\_pdupl} = \frac{n_{data}}{n_{data} + 8}. \tag{1.6}$$

Summary

Table 1.2 summarizes the reviewed interfaces and their configurations for wired communication with body sensors. Among the interfaces considered in this study, those with push-pull transistor outputs (UART, SPI) are potentially more suitable than the popular I2C interface. This is because the operation of UART and SPI interfaces is less affected by parasitic parameters introduced by wire length and the amount of devices connected to the network.

Table 1.2

Compilation of low-power MCU communication interfaces for communication in the body sensor network

Interface	Configuration	Topology	Output	Wires	Symbol rate, kBd/s
I2C	Standard	↔Bus	OD/OC	2	100
I2C	Fast	↔Bus	OD/OC	2	400
I2C	Fast+	↔Bus	OD/OC	2	1000
I2C	High speed	↔Bus	OD/OC	2	3400
I2C	Ultra fast	↔Bus	PP	2	5000
UART	Address bit	⇆Bus	PP	2[a]	460,8[b]
UART	Idle frames	⇆Bus	PP	2[a]	460,8[b]
SPI	Full duplex	⇆Bus	PP	3+n_{nodes}[a]	1000[b]
SPI	Daisy-chain	⇆Line	PP	4	1000[b]
SPI	Half-duplex	↔Bus	PP	3	1000[b]
SPI	Enhanched SPI daisy-chain [9]	←Line	PP	2	1000[b]

↔ Half-duplex, ⇆ full duplex, ← simplex.
OC – open collector.
OD – open-drain.
PP – push-pull.
n_{nodes} – connected nodes.
[a] Half duplex configuration requires one less wire.
[b] A typical value for low-power MCUs commonly used nowadays.

The efficiency of data transmission in half-duplex configuration for the observed MCU interfaces, as a function of the number of data symbols n_{data}, is illustrated in Fig. 1.2.

1.5. Conclusions

To achieve precise reconstruction of body shape in challenging environmental conditions with low visibility and object occlusions, technologies that utilize orientation sensors at-

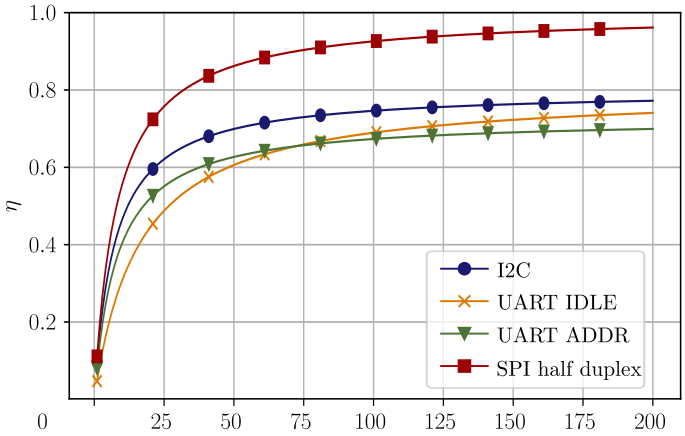

Fig. 1.2. The data transmission efficiency of the observed I2C, UART, and SPI interfaces using half-duplex bus configurations with a symbol transmission rate of $f_b = 460800Bd/s$.

tached to the body have been identified as the most suitable option.

The present techniques for shape reconstruction using orientation sensors attached to the body involve obtaining surface tangential information samples, interpolating the data, and numerically integrating the interpolated data based on the known geodesic distances between sensors. While the theoretical model acknowledges that the geodesic distances between sensors may change during stretching, this aspect is typically fixed in practical applications. In the literature review, devices that are suitable for reconstructing the shape of stretchable objects were not found. However, this is a crucial aspect to consider when creating systems that can fit and accurately reconstruct the shape of objects of various sizes.

Although wireless communication solutions are dominant among BSNs, for applications with a large number of densely deployed nodes, wired solutions may be more suitable. After a detailed examination of multiple low-power MCU communication interfaces, it was concluded that although I2C is currently utilized in several applications, interfaces with push-pull transistor outputs (UART, SPI) are potentially more suitable for BSNs. This is because they are less affected by parasitic parameters introduced by wire length and the devices connected to the bus.

Wired interfaces that use individual addressing methods have significant overhead proportional to the number of nodes from which data is retrieved. This limitation is particularly problematic for real-time body shape reconstruction systems that require efficient communication with a large number of functionally equivalent sensor nodes. Therefore, it is essential to develop an improved approach that reduces communication overhead in such systems.

2. METHOD FOR SHAPE RECONSTRUCTION WITH ORIENTATION SENSORS IN STRUCTURES

The goal of this Chapter is to introduce a novel approach to reconstructing the geometric shape of the body from orientation sensor data, which does not require specialized sensors to measure changes in geodesic distance between IMUs when the body is stretched.

2.1. The essence of the proposed method

The proposed method for body shape reconstruction using orientation sensors is characterized in Fig. 2.1. The curve $\boldsymbol{C}_{\mathbf{b}}(s_{\mathrm{b}})$ characterizing the body shape is connected with the curve characterizing elastic structure $\boldsymbol{C}_{\mathbf{a}}(s_{\mathrm{a}})$ in connection points $\boldsymbol{C}_{\mathbf{b}}(s_{\mathrm{b},m}) = \boldsymbol{C}_{\mathbf{a}}(s_{\mathrm{a},m})$, where $s_{\mathrm{a}} \in [0,L_{\mathrm{a}}]$ and $s_{\mathrm{b}} \in [0,L_{\mathrm{b}}]$ are curve arc-length parameters; $m = 1,2,...,M$ is connection point order number; M is total number of connection points; and L_{a}, L_{b} is total length of corresponding curves. On the structure in fixed points, $\boldsymbol{C}_{\mathbf{a}}(s_{\mathrm{a},k})$ are distributed orientation sensors, where $k = 1,2,...,K$ is sensor order number and K is the total number of sensors. The proposed method is based on the concept that when the body undergoes deformation by bending or stretching, the shape of the structures attached to the body changes accordingly. However, the overall length of the structure and geodesic distances between sensor points can remain constant within a certain range of body deformation.

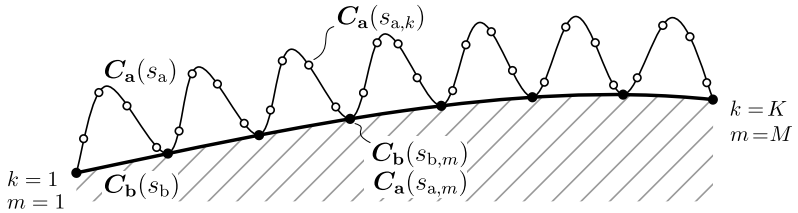

Fig. 2.1. A schematic diagram for body shape reconstruction using orientation sensors and a structure connected to the body at fixed points. $\boldsymbol{C}_{\mathbf{a}}(s\mathrm{a})$ – curve representing the structure, $\boldsymbol{C}_{\mathbf{b}}(s\mathrm{b})$ – curve representing the body shape, $\boldsymbol{C}_{\mathbf{a}}(s\mathrm{a},k)$ – the points representing the locations of the orientation sensors, $\boldsymbol{C}_{\mathbf{b}}(s\mathrm{b},m)$ – the connection points common to the mesh structure and the body, $k = 1,2,...,K$ – the order number of the sensor, K – the total number of sensors, $m = 1,2,...,M$ – the order number of the connection, and M – the total number of connections.

The proposed approach for reconstructing the body shape is based on the determination of the curve that characterizes the shape of the structure $\boldsymbol{C}\mathbf{a}(s\mathrm{a})$ using orientation data obtained from known locations $s_{\mathrm{a},k}$. The methods presented in Section 1.1 can be employed for this purpose. When the arc-length parameter values for the connection points $s_{\mathrm{a},m}$ are available, the determination of the coordinates for the points characterizing the body shape and the reconstruction of the body shape can be accomplished through

the use of chord length or centripetal parametrization, as discussed in [8]. In order to reconstruct the surface, the global surface reconstruction method described in [7] can be applied.

2.2. The properties of the proposed method

The current state-of-the-art approaches for body shape reconstruction using orientation sensors placed directly on the body are prone to accumulating reconstruction errors due to the inadequate number of sensors, as shown in Fig. 2.2 a. In contrast, the proposed method in the Thesis, as illustrated in Fig. 2.2 b, provides precise reconstruction of the given curve at the connection points, even if the reconstructed curve between these points significantly deviates from the given curve. This is irrespective of the arc-length distance to the origin of the reconstruction where $s = 0$. This peculiarity becomes more apparent when the shape of the structure is more suitable for interpolation and reconstruction using the methods described in Section 1.1, rather than the body shape itself.

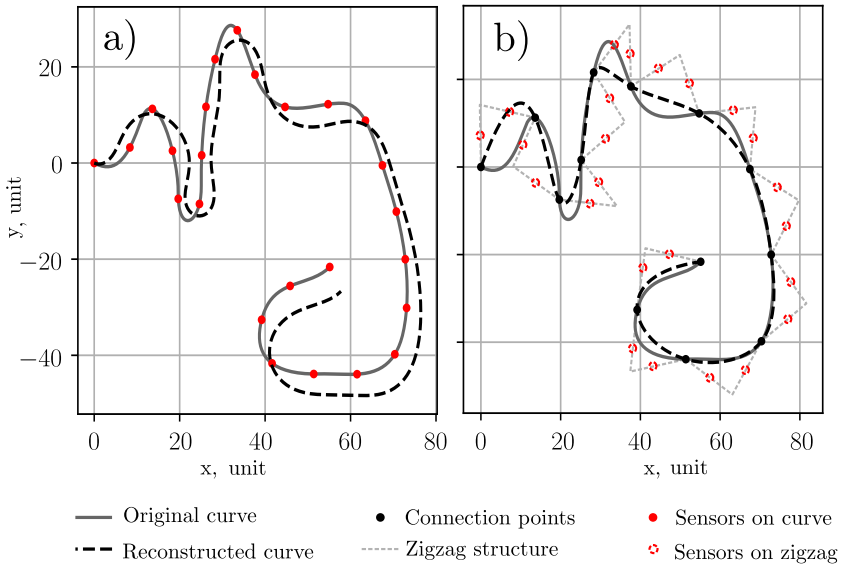

Fig. 2.2. Synthetically generated 2D lines reconstructed with ideal sensor readings: a) when sensors are on the line and b) when sensors are on a zigzag structure.

The allowable range of body shape variations for the proposed approach is determined by the mechanical properties of the structure. Firstly, the chord distance between connection points cannot exceed the length of the corresponding segment of the structure. Secondly, the mechanical realization of the structure imposes further limitations, such as its flexibility, physical dimensions, and interaction with solid objects.

In the process of constructing structures for body shape reconstruction, it is possible to strategically join certain connection points of the structure in order to create curve inter-

sections. As illustrated in Fig. 2.3, these intersections can be utilized to compensate for any potential reconstruction errors $\boldsymbol{D}_{\mathbf{off}}(s_{1,m})$, thereby improving the overall consistency and accuracy of the curve reconstruction process.

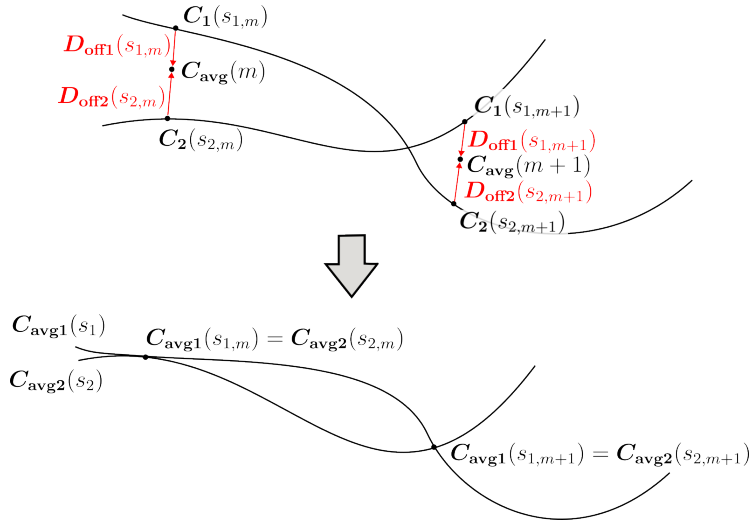

Fig. 2.3. Intersection offset compensation for structures with shared connection points. $\boldsymbol{C_1}(s_{1,m})$ and $\boldsymbol{C_2}(s_{2,m})$ – intersection points, $\boldsymbol{D}_{\mathbf{off}}(s_{1,m})$ – intersection offsets.

To calculate the true value between different estimates $\boldsymbol{C_1}, \boldsymbol{C_2}$,..., a weighted average is used:

$$\boldsymbol{C}_{\mathbf{avg}}(\boldsymbol{C_1}, \boldsymbol{C_2}, ...) = \frac{w_1 \boldsymbol{C_1} + w_2 \boldsymbol{C_2} + ...}{w_1 + w_2 + ...}, \tag{2.1}$$

where w – weights correspond to the distance of the point to the origin of reconstruction.

The offset vectors are obtained as follows:

$$\boldsymbol{D}_{\mathbf{off1}}(s_{1,m}) = \boldsymbol{C}_{\mathbf{avg}}(m) - \boldsymbol{C_1}(s_{m,1}), \tag{2.2}$$

$$\boldsymbol{D}_{\mathbf{off2}}(s_{2,m}) = \boldsymbol{C}_{\mathbf{avg}}(m) - \boldsymbol{C_2}(s_{m,2}). \tag{2.3}$$

The offset vectors $\boldsymbol{D}_{\mathbf{off1}}(s1,m)$ and $\boldsymbol{D}_{\mathbf{off2}}(s2,m)$ are obtained by interpolation to derive curve offsets $\boldsymbol{D}_{\mathbf{off1}}(s_1)$ and $\boldsymbol{D}_{\mathbf{off2}}(s_2)$. These offsets can be utilized to correct line points and adjust the coordinates of the connection point as follows:

$$\boldsymbol{C}_{\mathbf{avg1}}(s_1) = \boldsymbol{C_1}(s_1) + \boldsymbol{D}_{\mathbf{off1}}(s_1), \tag{2.4}$$

$$\boldsymbol{C}_{\mathbf{avg2}}(s_2) = \boldsymbol{C_2}(s_2) + \boldsymbol{D}_{\mathbf{off2}}(s_2). \tag{2.5}$$

2.3. A special case with zigzag structures

In this section a detailed examination of zigzag structures affixed to the body is undertaken, as depicted in Fig. 2.4.

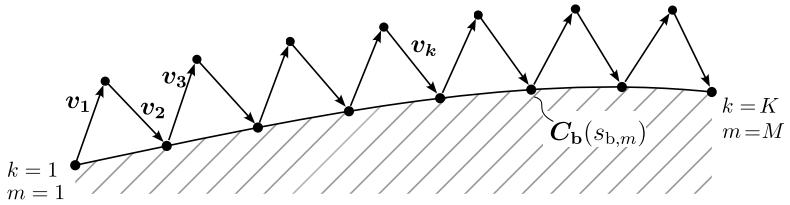

Fig. 2.4. A zigzag structure for 2D shape reconstruction of an object subjected to stretch and bend deformations.

The zigzag structures are represented by vectors $\boldsymbol{v_k}$ of a certain length $L_k = ||\boldsymbol{v_k}||$, along with attachment points $\boldsymbol{C_b}(s\text{b},m)$. The attachment point coordinates can be computed by exploiting the rotation matrices $\boldsymbol{R_k}$ associated with each zigzag segment, which describe their orientation with respect to specified reference states $\boldsymbol{v_k^*}$. Specifically, the attachment point coordinates can be calculated as follows:

$$\boldsymbol{C_b}(s_{b,1}) = \begin{bmatrix} 0 \\ 0 \end{bmatrix}, \tag{2.6}$$

$$\boldsymbol{C_b}(s_{b,m}) = \sum_{k=1}^{2(m-1)} \boldsymbol{v_k} = \sum_{k=1}^{2(m-1)} \boldsymbol{R_k v_k^*}, \quad \text{where} \quad m > 1. \tag{2.7}$$

In the 2D scenario, the reference state can be established along the horizontal axis. Specifically, the reference vectors can be represented as $\boldsymbol{v_k^*} = [L_k, 0]^\intercal$, and the coordinates of the attachment points can be expressed as follows for cases where $m > 1$:

$$\boldsymbol{C_b}(s_m) = \sum_{k=1}^{2(m-1)} \boldsymbol{R_k v_k^*} = \sum_{k=1}^{2(m-1)} L_k \begin{bmatrix} \cos(\alpha_k) & -\sin(\alpha_k) \\ \sin(\alpha_k) & \cos(\alpha_k) \end{bmatrix} \begin{bmatrix} 1 \\ 0 \end{bmatrix} = \sum_{k=1}^{2(m-1)} L_k \begin{bmatrix} \cos\alpha_k \\ \sin\alpha_k \end{bmatrix}, \tag{2.8}$$

where α_k is the angle between structure vectors and horizontal axis.

The use of zigzag structures can be extended to the reconstruction of connection points that define a 3D surface $\boldsymbol{C}(u,v)$, where u and v are used for the surface parametrization (2.5). The 3D points of the surface can be computed with respect to both the reference column $\boldsymbol{C}(0,v)$ and the reference row $\boldsymbol{C}(u,0)$, and the results may vary due to reconstruction errors. Hence, the knowledge of the connection points can be leveraged to reconcile the estimations based on the principle discussed previously and shown in Fig. 2.3.

The length of zigzag structure segments determines the extent of deformation, such as bending, stretching, and compressing, that the structure can endure. In the case of the structure depicted in Fig. 2.4, which features two zigzag segments between connection

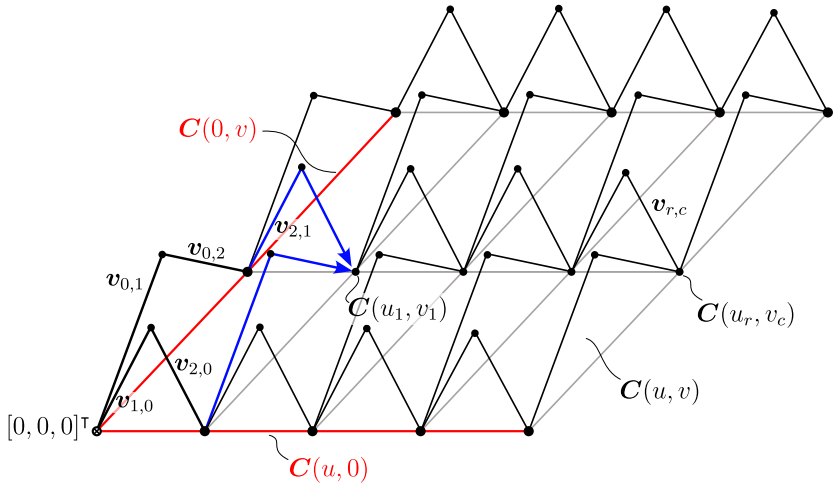

Fig. 2.5. Using spatial zigzag structures to obtain coordinates of points on body surfaces: an example of point acquisition with respect to reference row and column, as indicated by the blue lines for the point $\boldsymbol{C}(u_1, c_1)$.

points, the admissible chord lengths are given by $d_m \leq L_{2m-1} + L_{2m}$, where $m = 2,3,...,M$ and M is the number of connection points.

2.4. Conclusions

The utilization of IMUs in reconstructing the shape of stretching and bending deformed objects in structures connected to discrete points of the body presents several advantages over the approaches considered in this study, where IMUs are placed directly on the surface of the body. Firstly, the proposed approach allows for the distance between the connection points of the body and the structure to vary within certain limits without affecting the sensor geodesic distances on the structure, thus eliminating the need for additional sensors to read them independently. Secondly, the reconstruction error associated with an insufficient number of sensors to accurately interpolate the acquired tangential readings of the body shape can be reduced by constructing structures from geometric shapes, like zigzag, that are more accurately interpolated than the shape of the body itself.

3. PROPOSED APPROACH FOR BODY SENSOR DATA ACQUISITION

This Chapter presents a detailed description of an approach proposed for the acquisition of BSN data for body shape reconstruction.

3.1. Overall system architecture

Fig. 3.1 illustrates the system architecture designed to acquire sensor node data on a personal mobile device. The architecture consists of a large number of sensor nodes that are distributed all over the body, wired connections, a retransmission node with a power supply, and the mobile device itself, which serves as the platform for data aggregation and processing.

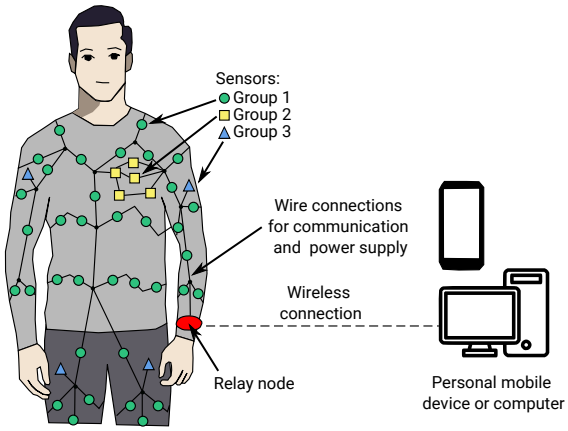

Fig. 3.1. The overall architecture of the proposed system.

To ensure a high degree of integration of electronic components, the network nodes utilize commercially available low-power integrated components, such as MEMS IMU sensors and MCUs. These components commonly use communication interfaces such as I2C, SPI, and UART, which are discussed in detail for communication in a bus topology in Section 1.4.

Reconstructing shape with orientation sensors requires reading a potentially large number of nodes simultaneously. In this case, it is more efficient to address grouped sensors as a whole, rather than individual sensors. To improve the performance of the proposed KST architecture with grouped sensors, a novel communication approach is proposed in Section 3.2. This approach replaces individual node addressing with a customized addressing protocol designed for groups of sensors.

3.2. Protocol for wired communication

The proposed protocol for efficient acquisition of data from a group of sensors, illustrated in Fig. 3.2, is composed of communication frames that form sequences of blocks containing addressing and sensor data.

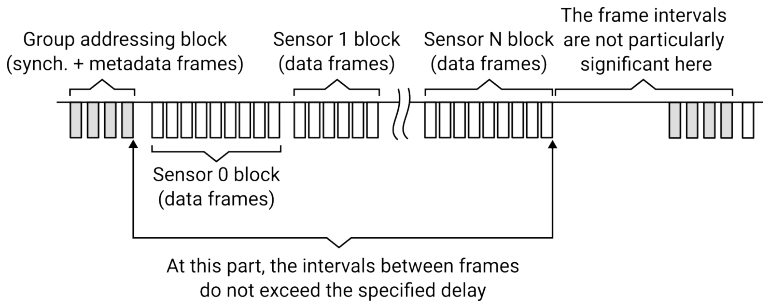

Fig. 3.2. Frame diagram of the proposed communication protocol.

The protocol utilizes the master-slave principle, where the master generates a unique addressing block for the group to be read. After transmission of the addressing block, the data is sampled, and the bus is considered busy while the sensor nodes of the group transmit their blocks of data in a specified sequence. To prevent the bus from hanging between frames, a time-out period is employed. Once this period has elapsed, all participating nodes assume that communication with the group has ended and the bus is available again.

With slight modifications, the proposed principle can be implemented for both UART and SPI bus half-duplex configurations:

1. For the UART half-duplex configuration, a unique sequence of synchronization frames can be arbitrarily chosen.

2. For the UART address bit configuration, a frame with an active address bit can be utilized for synchronization.

3. For the UART idle frame configuration, an idle frame can be employed for synchronization.

4. For the SPI in half-duplex configuration, the leading edge of the CS signal can be used for synchronization.

To compare with the protocols discussed in Section 1.4, we can evaluate the overhead reduction offered by the proposed protocol:

$$\mu = \frac{t_{overhead}}{t^*_{overhead}} = \frac{t_{protocol} - n_{data}/f_b}{t^*_{protocol} - n_{data}/f_b}. \tag{3.1}$$

The following results are obtained when applying individual addressing to groups of n_{nodes} nodes in SPI and UART half-duplex bus topologies:

$$\mu_{uart\_idle} = \frac{20 \cdot n_{nodes} + 0{,}25 \cdot n_{nodes} \cdot n_{data}}{20 + 0{,}25 \cdot n_{nodes} \cdot n_{data}}, \tag{3.2}$$

$$\mu_{uart\_addr} = \frac{11 \cdot n_{nodes} + 0{,}375 \cdot n_{nodes} \cdot n_{data}}{11 + 0{,}375 \cdot n_{nodes} \cdot n_{data}}, \tag{3.3}$$

$$\mu_{spi\_pdupl} = \frac{8 \cdot n_{nodes}}{8} = n_{nodes}. \tag{3.4}$$

As demonstrated, the proposed protocol reduces overhead by n_{nodes} times in the SPI half-duplex bus configuration, regardless of the amount of sensor data. The graphs in Fig. 3.3 provide a clearer illustration of the overhead reduction relationships for UART protocol configurations.

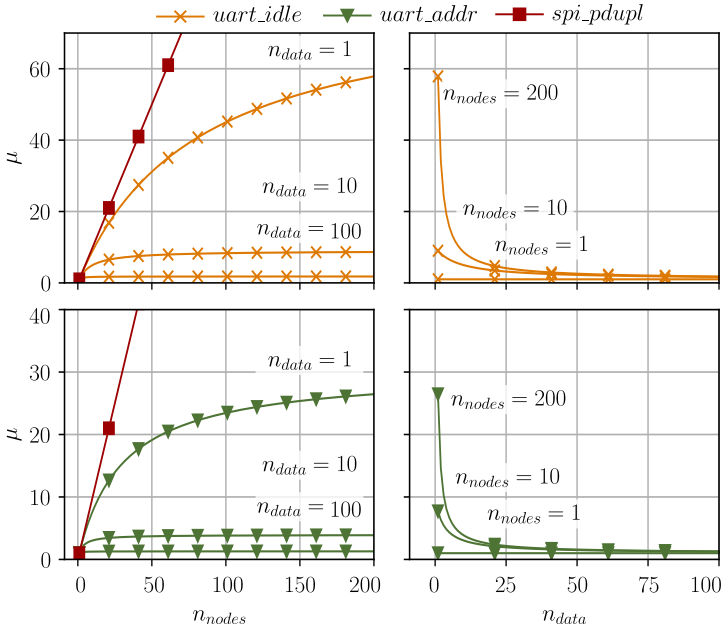

Fig. 3.3. The proposed protocol's overhead reduction for the UART and SPI half-duplex bus configurations depending on the number of nodes and the amount of data per node.

Although the reduction in overhead with the proposed protocol is significantly lower for UART configurations, there is still potential for significant overhead reduction in the UART idle frame format when the number of nodes is large and the amount of individual sensor data is small. In fact, the potential overhead reduction can be more than 10 times for cases where $n_{data} < 8$ and $n_{nodes} > 150$. Based on the relationships shown in the graphs of Fig. 3.3, the UART protocol could be a suitable choice for sensor networks where the number of nodes is large but the average amount of data per node is small. For instance, using UART idle frames, if $n_{data} < 24$ and $n_{nodes} > 25$, the value of μ would be greater than 3.8.

3.3. Architecture of BSN nodes

To specify the architecture of the BSN nodes for the proposed system designed for shape reconstruction of stretching and bending deformed bodies, the requirements for the nodes and wire connections (denoted as T in the table), sensor nodes (denoted as S in the table), and the relay node (denoted as R in the table) were defined and summarized in Table 3.1.

Table 3.1

Functional and operational requirements for the body sensor system for shape reconstruction of the body subjected to stretching and bending

No.	Requirements	Comments
T.1	Minimal amount of wired connections	For maximum ease of use and optimized material usage
T.2	Ability to create free wire connection branches from both the main unit and sensor nodes	To optimize material usage and improve the system's reliable operation
T.3	Minimal physical dimensions of nodes	Affects material usage and wearing comfort
T.4	Use of commercially available electronic components	Affects system costs and development complexity
T.5	Sensor data transmitted at 50 times per second	Corresponds to modern video standards, where the frame rate is usually synchronized with the industrial network frequency
S.1	Number of sensor nodes – up to 100 functionally identical nodes	Potential for detailed body shape reconstruction
S.2	Sensor nodes provide local orientation measurements	Requirement for the body shape reconstruction
R.1	Relay node provides power to all network nodes	Reduces sensor node size, complexity, and costs
R.2	Power source is rechargeable	Reduces hazardous waste
R.3	Uses widely available wireless technology in personal mobile devices for sensor data retransmission	No need for specialized equipment

To fulfil the specified requirements of the BSN, a physical network topology was proposed and is depicted in Fig. 3.4. This topology employs a UART half-duplex bus configuration and three wire connections, including Tx/Rx for asynchronous data signals, VCC for positive supply voltage, and GND for ground. For efficient data transfer and synchronous sampling, the protocol outlined in Section 3.2 is utilized. The schematic design of the sensor node and relay node using commercially available, low-power components is illustrated in Figs. 3.5 and 3.6, accordingly.

The proposed architecture for the system and its nodes has multiple advantages compared to other considered body sensor systems which are using wired connections:

1. The topology with a single wire data bus allows for flexible and optimized wire

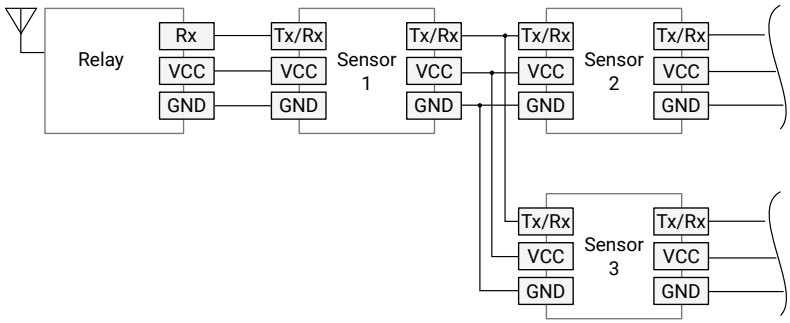

Fig. 3.4. Proposed physical network topology for BSN nodes.

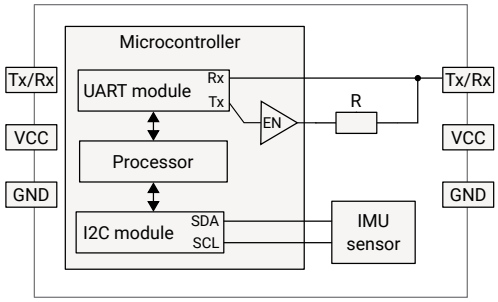

Fig. 3.5. Schematic design of the sensor node.

usage, reducing costs and improving the system's integration into clothing.

2. The bus signal encoding utilizing push-pull transistor outputs reduces signal distortion caused by wire parasitic parameters.

3. The proposed communication protocol for grouped sensor addressing reduces the overhead for sensor data readout.

3.4. Conclusions

To meet the system requirements for body shape reconstruction from orientation sensors, a new approach is proposed for acquiring sensor data from grouped sensors. A customized system architecture with wired connections and a new communication protocol for grouped sensors is proposed. This approach facilitates optimized wire usage, significantly reduces data overhead and improves efficiency for half-duplex configurations of SPI and UART. In particular, the overhead reduction is higher for SPI compared to UART and is proportional to the number of read nodes, regardless of the number of data symbols.

However, for applications that prioritize minimal wire usage, the UART half-duplex configuration may be more appropriate. After analysing the overhead reduction, the

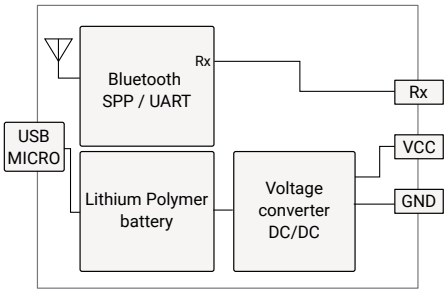

Fig. 3.6. Schematic design of wireless relay node.

results indicate that the proposed protocol for UART offers significant improvements in situations where the number of sensor data symbols is small (less than 24) and the number of sensors is large (more than 25).

To meet the functional and operational requirements of the system for body shape reconstruction, the network node architecture was adapted to use UART half-duplex configuration for communication. Compared to other known approaches for acquiring human body sensor data through wire connections, the proposed approach offers several advantages. The chosen network topology reduces wire usage and enhances flexibility in forming connections. The selected communication interface minimizes the impact of network parasitic parameters on signal quality, and the chosen protocol reduces symbol overhead in communication.

4. SIMULATIONS AND EXPERIMENTAL STUDIES

The objective of this Chapter is to validate the approaches described in Chapters 2 and 3 through numerical simulations and experimental studies.

4.1. Simulations for shape reconstruction

In order to evaluate the impact of several factors on the accuracy of the proposed method, a series of numerical simulations were conducted employing synthetic data from zigzag structures connected to randomly synthesized 2D curves. The factors under consideration encompassed 1) reconstructed body shape, 2) sensor placement frequency, 3) sensor measurement error, and 4) zigzag structure segment length. The outcome of the simulations facilitated the estimation of errors induced by the aforementioned factors. The findings of the study are applicable to 3D lines, presuming that the error vector length remains congruent with that obtained from the 2D analysis.

The simulation procedure is depicted in the block diagram shown in Fig. 4.1. 2D curves are synthesized by generating uniformly distributed random samples of an angle function with unit length, which are then interpolated using cubic splines to minimize the change in curvature of the angle function [16]. The curves are reconstructed by integrating the angle function, as demonstrated in Formula (1.1). The complexity of the angle function and the number of sensor samples required for its reconstruction depend on the number of random samples K_{gen}.

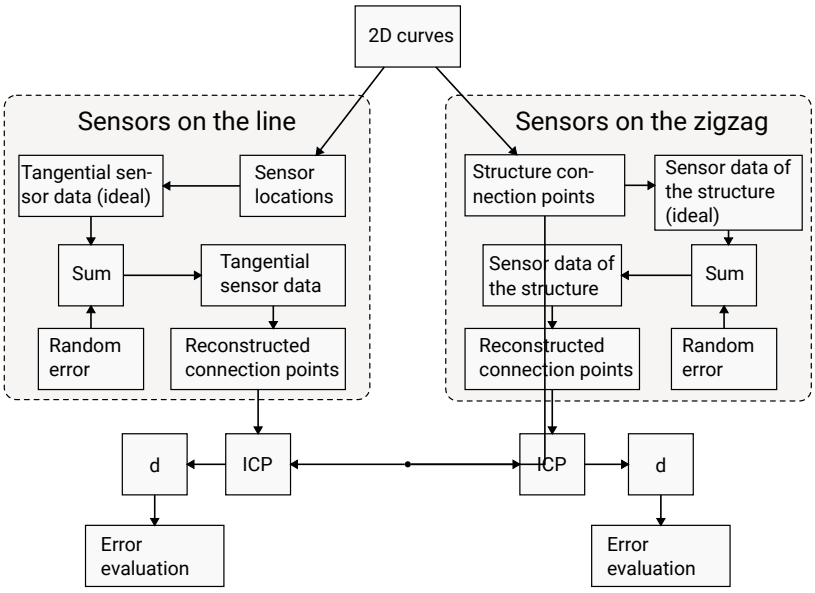

Fig. 4.1. Block diagram of shape reconstruction simulations.

In both approaches (sensors on a line and sensors on a zigzag), ideal sensor data is

synthesized as α_k – the angle between the sensor and the horizontal axis. The stretching coefficient $\lambda = s_{conn\_\max}/s_{conn} = 2L/s_{conn}$ is defined to characterize the stretching of the zigzag structure, where $s_{conn\_\max}$ is the maximum allowable distance between connection points of the structure.

In simulations prior to the reconstruction of the zigzag structure shape and connection points using the approach described in Section 2.3, the random error $\Delta\alpha_k$ is added to the sensor data to account for measurement uncertainty caused by real sensors.

The reconstructed connection coordinates are aligned with the reference coordinates using the iterative closest point (ICP) algorithm [6], and the reconstruction error between aligned 2D points is evaluated by calculating the Euclidean distance:

$$d = \sqrt{(x_1 - x_2)^2 + (y_1 - y_2)^2}, \tag{4.1}$$

where x_1, y_1 are coordinates of the reconstructed points and x_2, y_2 – coordinates of the reference points.

The simulation results for varying number of samples of the angle function K_{gen} are shown in Fig. 4.2[1]. The range of K_{gen} considered in this study spans from 4 to 24, while all other parameters remain fixed. As shown, the proposed method exhibits very low average error dependence on the number of generated points, in contrast to the approach where sensors are placed on a line, where the average error value increases rapidly when K_{gen} approaches and exceeds $n_{sens}/2$.

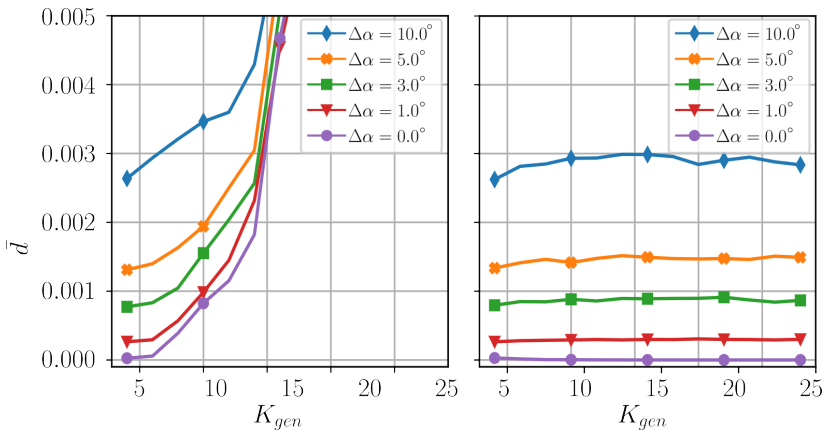

Fig. 4.2. The average error in reconstructing connection points as a function of the number of samples used for line synthesis: a) reconstruction with sensors on the curve that describes the shape of the body; b) reconstruction with sensors on the curve that describes the shape of the zigzag structure. Fixed parameters: $n_{sens} = 30$, $\lambda = 1$, $N_{rand} = 100$.

[1] `https://pubgit.edi.lv/armands-phd/simulations/-/blob/master/RandSim_2.py`

The simulation results with varying number of sensors n_{sens} and fixed other parameters are shown in Fig. 4.3[2]. As can be observed, using the proposed method in this dissertation, when $\Delta\alpha = 0$, the connection points are reconstructed perfectly. However, as the sensor error increases, the reconstruction error and its dependence on the number of sensors also increases.

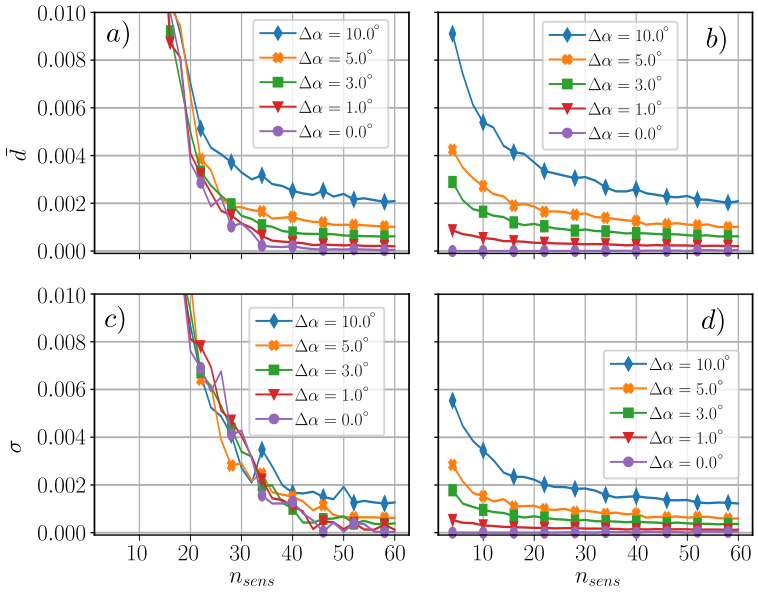

Fig. 4.3. The average error of reconstructed connection points depending on the number of sensors: a) reconstruction with sensors on the body; b) reconstruction with sensors on zigzag structures. The standard deviation of reconstruction errors σ: c) reconstruction with sensors on the body; d) reconstruction with sensors on zigzag structures. Fixed parameters: $K_{gen} = 10$, $\lambda = 1$, $N_{rand} = 100$.

The simulation results with varying stretch coefficient λ are shown in Fig. 4.4[3]. As can be seen in Fig. 4.4 b, there is a linear correlation between the stretch coefficient and the average error. Moreover, the slope of the curve increases as the sensor measurement error $\Delta\alpha$ increases. Therefore, to minimize the reconstruction error of connection points in the zigzag structure body shape reconstruction, it is recommended to use as small Zigzag segment lengths as possible.

4.2. The experimental set-up for hand shape reconstruction

In this Chapter, the design, development, and testing of an experimental model are described to verify the proposed system architecture (Section 3) and the approach for body

[2] `https://pubgit.edi.lv/armands-phd/simulations/-/blob/master/RandSim_1.py`
[3] `https://pubgit.edi.lv/armands-phd/simulations/-/blob/master/RandSim_2.py`

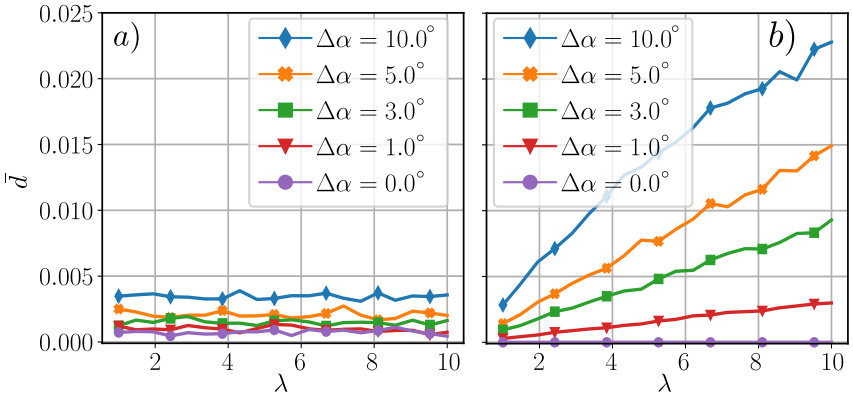

Fig. 4.4. The reconstruction error of connection points depending on the stretch factor of the zigzag structure: a) reconstruction with sensors on the body; b) reconstruction with sensors on zigzag structures. Fixed parameters: $K_{gen} = 10$, $n_{sens} = 30$, $N_{rand} = 100$.

shape reconstruction with IMUs (Chapter 2). Commercially available components, custom printed circuit boards, and 3D-printed parts were used to make the experimental set-up.

The experimental set-up, as shown in Fig. 4.5, contains a zigzag structure connected at fixed points to a tight-fitting clothing for reconstructing the shape of the arm (markers are attached to the connection points). The zigzag structure consists of 26 segments with a total length of 1.534 m and has 12 connection points with the body. After evaluating the accuracy of the zigzag joints, it is assumed that the endpoints of the segments coincide with an uncertainty of ±2.5 mm.

The development of the sensor network is based on the protocol described in Section 3.2 and the node architecture described in Section 3.3. Communication between nodes is achieved using a connection with 3 wires (GND, VCC, Tx/Rx) following the basic configuration of the UART half-duplex bus, and power is delivered through these same wires. The following UART frame format is used for asynchronous communication: 1 start and stop symbol, 0 parity symbols, 8 data symbols, and a symbol transmission rate of 460800 Bd/s.

The communication addressing block is formed by a fixed sequence of six UART frames: [0x55, 0xAA, 0x55, 0xAA, LEN(0-7), LEN(8-15)]. Data from each sensor is transmitted through the wire network using 12 frames, which include the sensor's identification number (ID) within the group, quaternion readings, the sensor's background calibration status, and cyclic redundancy check. Each sensor is assigned a unique ID associated with its location on the zigzag structure and the order in which sensor nodes send data after receiving the group addressing block.

Using the UART frame format, addressing block structure, and sensor data structure described above, the total number of frames required for sensor data acquisition is

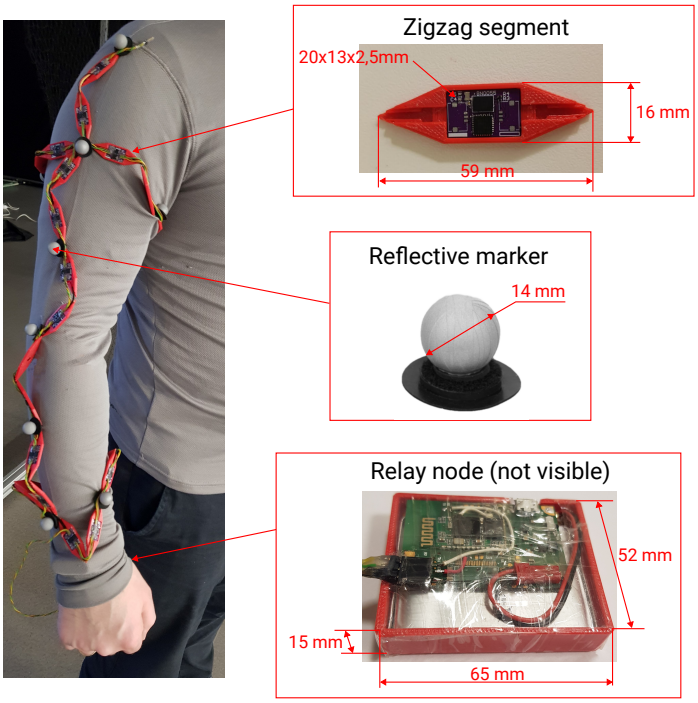

Fig. 4.5. Experimental set-up for arm shape reconstruction with zigzag structures.

$n_{frames} = 6 + n_{nodes} \cdot 12 = 6 + 26 \cdot 12 = 318$. Therefore, the minimum time required for transmitting all frames from all nodes in the experimental set-up is:

$$\min\{t_{frames}\} = n_{frames} \cdot 10/f_b = (6 + n_{nodes} \cdot 12) \cdot 10/f_b = \\ = 318 \cdot 10/460800 \approx 6.9 \text{ ms} \tag{4.2}$$

and the maximum frequency for transmitting all frames from the set-up:

$$f_{frames\_max} = \frac{1}{\min\{t_{frames}\}} \approx 144.9 \text{ Hz} \tag{4.3}$$

The complete design of the sensor nodes integrated into the zigzag segments is accessible on Gitlab.[4] The sensor nodes consist of a *BNO055* IMU chip and *MSP430G2553* MCU with firmware for which the Code Composer Studio project with C code is available on Gitlab.[5]

The program for the first sensor (ID = 0) has been modified to function as the master node and generate the communication initiation sequence at a fixed time interval (20 ms). Accordingly, the Code Composer Studio project with C code for the modified sensor master node program for the BNO055 microcontroller can be found on Gitlab.[6]

[4] `https://pubgit.edi.lv/armands-phd/sensor-node-pcb`
[5] `https://pubgit.edi.lv/armands-phd/sensor-node-bus-fw`
[6] `https://pubgit.edi.lv/armands-phd/sensor-node-bus-fw/-/tree/master-node`

The wireless transmission node was implemented according to the block diagram shown in Fig. 3.6. It uses a UART/Bluetooth module for wireless communication, and the datasheet for the module is available online.[7] To provide a stable 3.3 V power supply, the node contains a 2000 mAh lithium-polymer battery and a switching voltage regulator.

4.3. Evaluation of communication protocol

To evaluate the performance of the developed experimental wire communication protocol, the "Tx/Rx" data signal during protocol operation was analyzed using the "DSLogic U3Pro16"[8] logic analyzer (sampling frequency of 1 GHz), which determined the time intervals shown in Fig. 4.6: t_1 – time for group addressing block; t_2 – time for obtaining local sensor readings; t_3 - time for transmitting sensor data blocks after all local sensor readings have been obtained; t_4 – time for which the network is idle. The sum of all these times constitutes the sensor data reading period $T = t_1 + t_2 + t_3 + t_4$. In addition, the number of sent frames was recorded in each time interval to calculate the average time t_{frame} required to reject one frame. The obtained results, by measuring 10 consecutive group readings, are summarized in Table 4.1.

Table 4.1

Results of protocol time interval measurements

Time	Average	Standard Deviation	Minimum	Maximum
t_1	130.73 µs	0.016 µs	130.720 µs	130.770 µs
t_2	3.13 ms	0.396 ms	1.978 ms	3.480 ms
t_3	6.56 ms	0.247 ms	6.019 ms	7.124 ms
t_4	10.28 ms	0.302 ms	9.880 ms	10.821 ms
T	20.11 ms	0.141 ms	20.045 ms	20.517 ms
t_{1_frame}	21.79 µs	0.003 µs	21.787 µs	21.795 µs
t_{3_frame}	22.79 µs	0.018 µs	22.771 µs	22.833 µs

As shown in Table 4.1, the frame transmission times t_{1_frame} and t_{3_frame} are very close to the maximum possible value: $t_{frame} = 10/460800 = 21.70$ μs. Consequently, due to delays in the microcontroller program, the time overhead in the data transmission phase (t_3) amounts to about 5 %. However, without decreasing the network sampling frequency (50 Hz), the number of sensor nodes that can be connected and read in the network can be increased by up to $\lfloor (t_{4\,\min}/t_{3frame\,\max} - 6)/12 \rfloor = 35$, allowing for up to 61 sensor nodes to be supported in the network.

[7] `https://components101.com/sites/default/files/component_datasheet/HC-05%20Datasheet.pdf`

[8] `https://www.dreamsourcelab.com/shop/logic-analyzer/dslogic-u3pro16/`

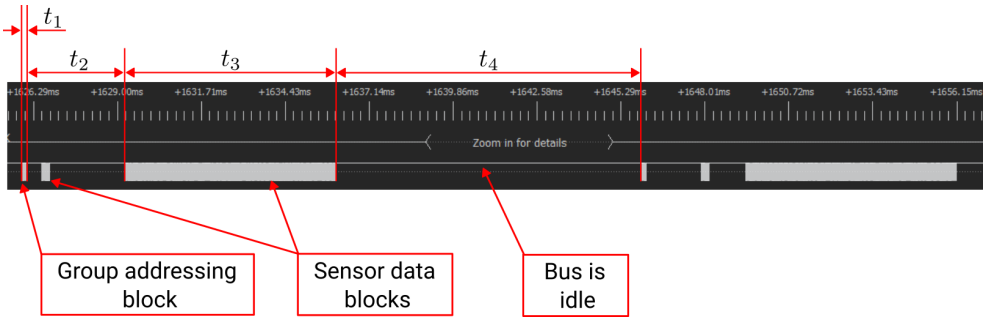

Fig. 4.6. Experimental setup's digital signal screen-shot of data lines.

Using the data from Table 4.1, we can also estimate the maximum frame transmission frequency for the prototype as $f^*_{frames_{\max}} = \frac{1}{t_{1\,\max}+t_{2\,\max}+t_{3\,\max}} \approx 93$ Hz, which is approximately 64 % of the theoretically possible frequency with the protocol used.

4.4. Evaluation of reconstruction accuracy for connection points

To evaluate the precision of the developed experimental set-up's connection point reconstruction, the coordinates of the connection points obtained using a zigzag structure were compared with the marker coordinates obtained with the Optitrack™ optical marker tracking system.

The experiment utilized the following devices, as depicted in Fig. 4.7: a personal computer, the zigzag structure experimental set-up with 12 connection points for hand shape reconstruction described in Section 4.2, an Optitrack system equipped with 8 infrared cameras and 12 reflective markers with a 14 mm diameter attached to the connection points of the zigzag structure. Due to the physical size of the markers, the coordinates of the Optitrack marker centres and the coordinates of the attachment points obtained with the zigzag structure are assumed to coincide with a ± 7 mm uncertainty, which corresponds to the radius of the reflective markers.

During the experiment, the experimental set-up of the zigzag structure was filmed using the Optitrack camera system while the user assumed various static poses at predetermined time intervals (10 s). Three basic static hand poses were selected and repeated in as many different directions as possible. The basic poses are as follows:

- Straight arm (Pose 1): The arm and palm are fully extended in a straight line. This pose allows for the validation of the system for reconstructing relatively simple shapes.
- Straight and rotated arm (Pose 2): The arm is extended just like in Pose 1, but the palm is rotated 180 degrees. This pose allows for the validation of the system for reconstructing twisted shapes.
- Bent arm (Pose 3): The arm is bent at the elbow, forming a right angle. This pose

involves rapid changes in body shape in the elbow joint region, allowing for the validation of the system for reconstructing body shape with joints.

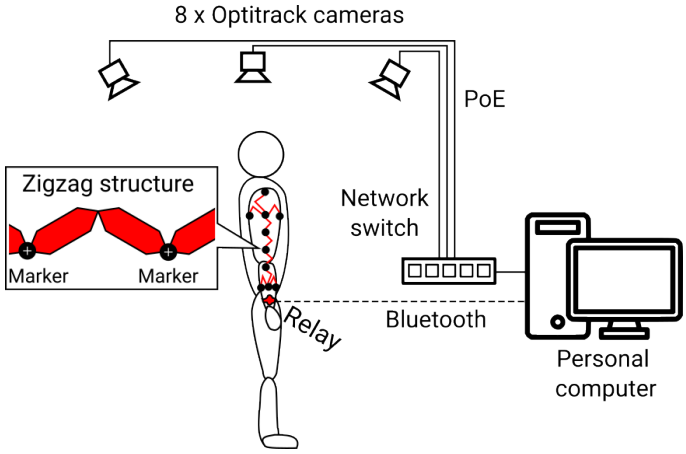

Fig. 4.7. Experimental installation for evaluating the precision of reconstructing the connection points of the experimental zigzag structure set-up.

The Optitrack™ software "Motive 3.0.1 Final" (June 7, 2022)[9] was used for recording and preprocessing (point labeling) Optitrack data. The processed data frames and corresponding time stamps were then exported to a comma-separated values (CSV) file. Additionally, a special tool[10] was developed for recording the sensor data of the experimental set-up of the zigzag structure. This tool provides the acquisition of IMU data frames and saves the frames in CSV format with corresponding time stamps.

The approach described in Section 2.3 was utilized for reconstructing the connection points of the zigzag structure from BNO055 sensor orientation data. The relative coordinates of the attachment points obtained from the structure and the measurements obtained from Optitrack were aligned using the ICP algorithm [6].

The Euclidean distances between the points determined by both systems are compiled in Table 4.2 and shown in Fig. 4.8. Taking all visible marker readings in all poses, the average distance between the points in the static pose case is 19.9 mm ±12.45 mm, which accounts for 0.8 % of the total length of the zigzag structure set-up (1.53 m). This difference can potentially be reduced by improving the precision of the connection points for the zigzag structure segments (±2.5 mm), reducing the offset between the zigzag structure connection points and Optitrack marker centres (±7 mm), and decreasing the mismatch between the local coordinate systems of the zigzag segments and the orientation sensor.

To evaluate the stretch coefficient of the experimental zigzag structure set-up in experiments, the average length of the line formed by chords between the connection points was

[9] `https://optitrack.com/support/downloads/motive.html`
[10] `https://pubgit.edi.lv/armands-phd/loggingtool`

Table 4.2

The difference in coordinates of the connection points obtained from the experimental set-up of the zigzag structure and the Optitrack marker tracking camera system (the values are indicated in millimetres).

Point No.	Pose 1		Pose 2		Pose 3		Overall	
	$\bar{d}$	σ	$\bar{d}$	σ	$\bar{d}$	σ	$\bar{d}$	σ
1	13.53	4.32	12.79	2.26	19.94	5.43	15.65	5.44
2	7.62	2.64	8.76	2.19	18.51	8.12	11.81	7.27
3	20.14	10.94	20.71	8.93	19.95	5.92	20.22	8.95
4	23.27	5.49	32.10	11.16	25.36	4.01	26.62	7.81
5	21.73	8.99	26.28	7.33	21.37	3.28	22.73	7.29
6	10.19	2.70	9.57	4.46	24.81	13.04	15.28	10.94
7	14.42	5.59	10.30	2.37	29.68	19.46	18.86	14.74
8	15.68	6.65	11.95	3.52	35.14	22.88	21.73	17.63
9	15.40	9.95	12.11	5.49	23.52	16.08	17.58	12.79
10	20.03	9.10	23.55	9.91	30.64	16.37	24.75	13.34
11	29.10	12.64	22.70	8.66	32.13	13.88	28.34	12.68
12	27.99	11.20	26.36	9.37	30.72	10.99	28.44	10.81
Overall	17.09	10.44	16.70	9.97	25.14	14.14	19.90	12.45

calculated: 980.9 mm ±21.78 mm. Therefore, the estimated average stretch coefficient of the structure is $\lambda_{\text{exp}} = 1534/980.9 \approx 1.56$. Taking into consideration the potential uncertainty in the BNO055 sensor measurement of $\Delta\alpha_{\text{BNO055}} = 4.61°$ [13], we can approximately estimate the simulated average error from the curves in Fig. 4.4, which represents the reconstruction error of the connection points on the line with unit length, $\bar{d}_1(\lambda = 1.56, \Delta\alpha = 4.61) \approx 0{,}025$. As a result, the average error of the experimental zigzag structure model's connection points, caused by the uncertainty in the BNO055 sensor measurement, is approximately 3.8 mm.

4.5. Conclusions

Simulations have shown that the proposed method for reconstructing connection points on body shapes is much less affected by the shape itself compared to approaches that utilize sensors directly on the body. It has also been discovered that the precision of connection point reconstruction is inversely proportional to the number of sensors in both cases. Furthermore, in the case of zigzag structures, the reconstruction error converges to zero as the measurement error of the sensors decreases, providing a significant advantage for applications where determining the necessary sensor placement on a line to obtain sufficient tangential information for interpolation is difficult, or where the complexity of the body shape makes its precise reconstruction with surface sensors practically unfeasible

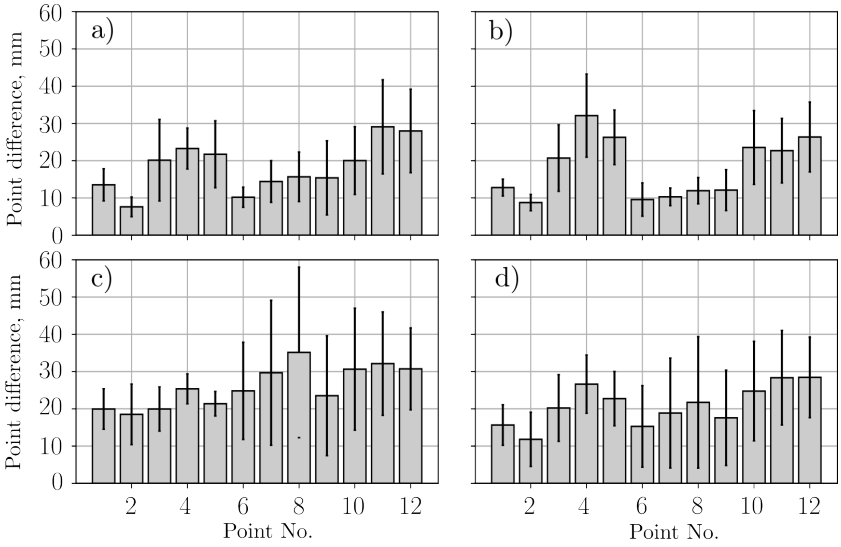

Fig. 4.8. Distance between the connection points of the zigzag structure set-up and Optitrack markers in the static object shape reconstruction. a) Pose 1: arm straightened; b) Pose 2: arm twisted; c) Pose 3: arm bent at the elbow; d) overall for all poses.

Simulations evaluating the impact of stretch coefficient on reconstruction precision revealed a linear correlation. Greater stretch coefficient and longer zigzag segments led to larger reconstruction error and sensor angle error influence. Selecting shorter zigzag segment lengths is recommended for real systems using the proposed approach.

A setup for experimental arm shape reconstruction has been developed, utilizing 26 zigzag segments to accurately determine the coordinates of 12 connection points along the arm's length. The orientation of the zigzag segments is acquired and transmitted to an external device at a frequency of 50 Hz, which can be increased up to 93 Hz to ensure visually smooth shape reconstruction. While this is only 64 % of the theoretically possible 144.9 Hz according to the protocol parameters, the sensor count or sampling frequency of the experimental model can be increased if necessary to meet the requirements of various applications.

When evaluating the reconstructed points of an experimental set-up against an Optitrack marker tracking system, it was found that the overall average difference for static poses was 19.9 mm. This could potentially be reduced to a limit of 3.8 mm, which was approximately estimated based on the parameters of the experimental model and simulations performed. Other identified causes of mismatch between these systems include imprecisions in the structure's connections (±2.5 mm), offset between the connection points and Optitrack marker centres (±7 mm), and discrepancies between the local reference systems of the zigzag segments and the sensor chips.

5. CONCLUSION. THE MAIN RESULTS AND CONCLUSIONS OF THE WORK.

The aim of this work is to design and develop a scalable and efficient body sensor system that can accurately reconstruct stretchable and bendable body shapes. The accomplishment of the assigned tasks to achieve the goal, along with the resulting findings and conclusions, are outlined in four Chapters of the Thesis.

In Section 1.1 of the Thesis, various methods for determining body shape are summarized and compared. Among them, an approach utilizing orientation sensors placed on the body is considered the most promising for reconstructing body shape with high precision. This approach can be applied not only to bodies subjected to bending, but also to those that undergo stretching deformation, provided that the inter-sensor distances are determined in addition to IMU spatial orientations each time. However, in the reviewed literature, the implementation of such systems with varying inter-sensor distances has been sparsely investigated, and no specific examples of implementation have been offered.

In the Thesis (Chapter 2), a new approach is proposed for reconstructing points characterizing the shapes of stretchable and bendable bodies. The proposed approach is based on placing orientation sensors not on the body surface, but on zigzag structures connected to the body at separate points. Compared to the reviewed literature, besides the ability to determine the shapes of stretch-deformed bodies without additional measurements of changes in inter-sensor distances, another significant potential advantage of the proposed method is that the precision of the reconstructed connection points is less affected by the body shape to be determined.

By conducting simulations using randomly generated synthetic curves and synthetic orientation sensor data (Section 4.1), the hypothesis proposing the reduction of body shape influence on reconstruction results was confirmed. Moreover, the simulations evaluated the impact of the number of sensors on the precision of reconstructed connection points. In contrast to the approach of placing sensors directly on the body, the proposed method converges the reconstruction error to zero, independent of the number of sensors, as the measurement error decreases. The simulations also assessed the effect of zigzag structure segment length on the precision of reconstructed connection points, revealing a direct proportionality between the segment length and average reconstruction error. Therefore, in real-world applications, it is advisable to minimize the length of structure segments to diminish the error in reconstructing connection points.

Taking into account the potentially large number of sensors required for detailed body shape reconstruction, relevant body sensor network communication technologies and their suitability for creating a large number of sensor networks were examined in Section 1.3. It was concluded that wireless solutions currently dominate, but for applications with a large number of densely deployed sensors, wired solutions are more suitable and are relatively unexplored in the context of body sensor networks.

Chapter 3 of the Thesis introduces a novel approach that presents a detailed descrip-

tion of collecting data from a large number of densely deployed nodes in a body sensor network. The proposed approach is based on wired connections and interfaces with push-pull transistor outputs (UART, SPI) that are commonly found in low-power MCUs. The approach includes a customized wired network architecture with three wire connections (data signal and power delivery) suitable for optimized node physical topologies, as well as a communication protocol that considerably enhances symbol transmission efficiency for grouped sensors. It was determined that the proposed communication protocol can reduce group communication overhead proportionally to the number of grouped nodes.

To evaluate the proposed methods for data acquisition and body shape reconstruction through practical experiments, an experimental device was developed with a zigzag structure to reconstruct the shape of the arm. The device consists of 26 zigzag segments with IMUs, which create 12 connection points with the body. The proposed approach for data acquisition and power supply of the sensors was implemented using 3-wire connections in a bus topology. Upon analysing the communication signal, it was determined that the orientation data of all 26 sensor nodes can be obtained from the device at a rate of up to 93 times per second. This is equivalent to approximately 64 % of the theoretical maximum speed with the protocol parameters used. Based on these results, it is affirmed that the proposed approach for acquiring body sensor data from a large number of densely deployed sensors can be achieved using commercially available low-power components and is suitable for real-time systems.

In comparing the experimental device developed in the Thesis with the Optitrack marker tracking system for reconstruction of various body postures, the average difference between the obtained connection point coordinates is ± 19.9 mm. It was identified that most of this discrepancy is due to imprecisions in segment connections (± 2.5 mm), Optitrack marker center offsets (± 7 mm), and the uncertainty of the sensor chip measurements (± 3.8 mm). Therefore, it can be concluded that the experimental study validates the suitability of the proposed approach for determining coordinates of points on the body surface and reconstructing body shape.

In general, the simulations and experiments carried out confirm the suitability of the proposed method for reconstructing body shapes from orientation sensor data, and several advantages have been identified compared to other known methods. The proposed approach for sensor data acquisition in BSN, which includes the system architecture and communication protocol for obtaining body sensor data, can be easily scaled to different numbers of sensor nodes and complex physical topologies. It allows for optimizing the use of wires required to create the sensor network and data transmission overheads by utilizing low-power MCU communication interfaces.

Based on the accomplished tasks and attained results, it can be concluded that the objective set forth in the Doctoral Thesis has been achieved, the research study has been successfully completed, and the work has been finished.

REFERENCES

[1] Hermanis A., Cacurs R., and Greitans M. Acceleration and magnetic sensor network for shape sensing. *IEEE Sensors Journal*, 16(5): 1271–1280, 2016. Cited by: 25.

[2] A. Ancans, A. Rozentals, K. Nesenbergs, and M. Greitans. Inertial sensors and muscle electrical signals in human-computer interaction. volume 2017-December, pp. 1–6. Institute of Electrical and Electronics Engineers Inc., 2018. Cited by 9.

[3] Armands Ancans, Modris Greitans, Ricards Cacurs, Beate Banga, and Artis Rozentals. Wearable sensor clothing for body movement measurement during physical activities in healthcare. *Sensors*, 21(6), 2021.

[4] Armands Ancans, Juris Ormanis, Ricards Cacurs, Modris Greitans, Elise Saoutieff, Adrien Faucorr, and Sebastien Boisseau. Bluetooth low energy throughput in densely deployed radio environment. Institute of Electrical and Electronics Engineers Inc., 2019. Cited by: 8; All Open Access, Green Open Access.

[5] Csaba Antonya, Silviu Butnariu, and Claudiu Pozna. Real-time representation of the human spine with absolute orientation sensors. In *2016 14th International Conference on Control, Automation, Robotics and Vision (ICARCV)*, pp. 1–6, 2016.

[6] P. J. Besl and Neil D. McKay. A method for registration of 3-d shapes. *IEEE Transactions on Pattern Analysis and Machine Intelligence*, 14(2): 239–256, 1992.

[7] John Fisher, John Lowther, and Ching-Kuang Shene. Curve and surface interpolation and approximation. volume 36, page 146, 06 2004.

[8] Michael S. Floater and Tatiana Surazhsky. Parameterization for curve interpolation. In Kurt Jetter, Martin D. Buhmann, Werner Haussmann, Robert Schaback, and Joachim Stöckler, editors, *Topics in Multivariate Approximation and Interpolation*, volume 12 of *Studies in Computational Mathematics*, pp. 39–54. Elsevier, 2006.

[9] A. Hermanis, R. Cacurs, K. Nesenbergs, and M. Greitans. Efficient real-time data acquisition of wired sensor network with line topology. pp. 133–138. IEEE Computer Society, 2013. Cited by: 7.

[10] Atis Hermanis. *Shape sensing based on embedded sensors for mobile cyber-physical systems*. Doctoral Thesis, Riga Technical University, 2016.

[11] Takayuki Hoshi and Hiroyuki Shinoda. 3d shape measuring sheet utilizing gravitational and geomagnetic fields. In *2008 SICE Annual Conference*, pp. 915–920, 2008.

[12] Daniel Laidig and Thomas Seel. Vqf: Highly accurate imu orientation estimation with bias estimation and magnetic disturbance rejection. *Information Fusion*, 91:187–204, 2023. Cited by: 1; All Open Access, Green Open Access.

[13] Zhirong Lin, Yongsheng Xiong, Houde Dai, and Xuke Xia. An experimental performance evaluation of the orientation accuracy of four nine-axis mems motion sensors. In *2017 5th International Conference on Enterprise Systems (ES)*, pp. 185–189, 2017.

[14] Sarvenaz Salehi Mourkani. *IMU-based Suit for Strength Exercises: Design, Calibration and Tracking*. Doctoral Thesis, Technische Universität Kaiserslautern, 2021.

[15] Saguin-Sprynski N., Jouanet L., Lacolle B., and Biard L. Surfaces reconstruction via inertial sensors for monitoring. pp. 702–709, 2014. Cited by: 11.

[16] Sprynski N., David D., Lacolle B., and Biard L. Curve reconstruction via a ribbon of sensors. pp. 407–410, 2007. Conference name: 14th IEEE International Conference on Electronics, Circuits and Systems, ICECS 2007; Conference date: 11 December 2007 through 14 December 2007; Conference code: 73150.

[17] Gregory M. Nielson. -quaternion splines for the smooth interpolation of orientations. *IEEE Transactions on Visualization and Computer Graphics*, 10(2): 224–229, 2004. Cited by: 26.

[18] Xavier Righetti and Daniel Thalmann. Proposition of a modular i2c-based wearable architecture. pp. 802–805. Ieee Service Center, 445 Hoes Lane, Po Box 1331, Piscataway, Nj 08855-1331 Usa, 2010.

[19] Nathalie Saguin-Sprynski, Mikael Carmona, Laurent Jouanet, and Olivier Delcroix. New generation of flexible risers equipped with motion capture - morphopipe system. volume 3, pp. 1932–1941, 2016. Cited by: 3.

[20] Elise Saoutieff, Tiziana Polichetti, Laurent Jouanet, Adrien Faucon, Audrey Vidal, Alexandre Pereira, Sébastien Boisseau, Thomas Ernst, Maria Lucia Miglietta, Brigida Alfano, Ettore Massera, Saverio De Vito, Do Hanh Ngan Bui, Philippe Benech, Tan-Phu Vuong, Carmen Moldovan, Yann Danlee, Thomas Walewyns, Sylvain Petre, Denis Flandre, Armands Ancans, Modris Greitans, and Adrian M. Ionescu. A wearable low-power sensing platform for environmental and health monitoring: The convergence project. *Sensors*, 21(5): 1–21, 2021. Cited by: 7; All Open Access, Gold Open Access, Green Open Access.

[21] Nathalie Sprynski. *Reconstruction de courbes et surfaces à partir de données tangentielles*. Thesis, Université Joseph-Fourier - Grenoble I, July 2007.

Armands Ancāns was born in 1992 in Līvāni. He received a Bachelor's degree in Electrical Engineering in 2014 and a Master's degree in Electronics in 2016 from Riga Technical University. Since 2015, he has been with the Institute of Electronics and Computer Science, contributing to various national and European projects. He started his career as an electronics engineer; he is currently a researcher, focusing on the development and implementation of wearable sensors. His scientific pursuits are focused on gaining insights into human body functions and providing valuable feedback for applications in sports and medicine.